

1 Article

2 Investigation of mechanical tests for hydrogen 3 embrittlement in automotive PHS steels

4 Renzo Valentini ¹, Michele Maria Tedesco ², Serena Corsinovi ³, Linda Bacchi³ and Michele
5 Villa^{3*}

6 ¹ Department of Civil and Industrial Engineering, Pisa University, Pisa 56122, Italy; renzo.valentini@unipi.it

7 ² Centro Ricerche Fiat S.C.p.A, Turin 10135, Italy; michele maria.tedesco@crf.it

8 ³ Letomec srl, Pisa 56126, Italy; research@letomec.com, l.bacchi@letomec.com

9 * Correspondence: m.villa@letomec.com

10 Received: date; Accepted: date; Published: date

11 **Abstract:** the problem of hydrogen embrittlement in Ultra High Strength Steels is well known. Slow
12 Strain Rate, Four Points Bending and permeation tests were performed with the aim of
13 characterizing innovative materials with an ultimate tensile strength higher than 1000 MPa. The
14 hydrogen uptake, in case of automotive components, can take place during manufacturing process:
15 during hot stamping, due to the presence of moisture that at high temperature dissociates giving
16 rise to atomic hydrogen, or also during electrochemical treatments like cataphoresis. Moreover,
17 possible corrosive phenomena could be a source of hydrogen during automobile life.

18 A test campaign was performed in order to characterize two innovative Press Hardened Steels
19 (PHS), USIBOR 1500 ® and USIBOR 2000 ®, and to establish a correlation between ultimate
20 mechanical properties and critical hydrogen concentration.

21 **Keywords:** Hydrogen Embrittlement, Ultra High Strength Steels, Automotive, Press Hardening
22 Steels, Hydrogen Induced Delayed Fracture, Diffusible Hydrogen
23

24 1. Introduction

25 The priority of maintaining and, if possible, increasing the safety of drivers and passengers
26 collides with the necessity of reducing the CO₂ emissions and so the weight of vehicles. In this contest
27 the research and characterization of new materials with the possibility of emissions reduction are
28 more and more diffused. To reduce thicknesses of sheets, higher tensile properties are required and
29 a major hydrogen susceptibility is the natural consequence.

30 Advanced high strength steels (AHSS) exhibit considerable mechanical properties and a good
31 formability and during the production process hydrogen could be adsorbed in various phases:
32 pickling, electroplating, cataphoresis and phosphating or even moisture during welding or heat
33 treatment, can cause an introduction of hydrogen in the material.

34 Press Hardened Steels (PHS) are hot formed steels and used in automobile structural and safety
35 components and present high homogeneity of mechanical properties and excellent fatigue resistance:
36 their manufacturing process consists mainly of an austenitizing of blanks in a oven and following
37 martensitic quenching in the water-cooled stamping tool.

38 The main source of hydrogen for this kind of materials is the hot stamping process: hydrogen comes
39 from the dissociation of water at high temperature, adsorption and absorption in the steel bulk and
40 its entrapment after water-cooling quenching.

41 The hydrogen present in the material can diffuse and concentrate in microstructural vacancies or
42 defects and crack the material giving rise to the so called Internal Hydrogen Embrittlement (IHE),
43 related to hydrogen charging before service.

44 The most known mechanisms that try to explain the interaction and behavior of hydrogen [1] with
45 steel are HEDE (Hydrogen Enhanced DEcohesion) and HELP (Hydrogen Enhanced Local Plasticity):

46 the first one assumes that hydrogen gives a contribution to the tensile strength: the higher the
 47 hydrogen concentration higher the hydrogen pressure and decohesion of steel atoms; the latter
 48 suggests that hydrogen, moving towards crack tips where hydrostatic stress is higher, promotes
 49 dislocations motion and reduces the interaction energy of them with internal obstacles with
 50 consequent formation of micro-voids.

51 Two different conditions were studied and compared in this work: on one side the Slow Strain Rate
 52 Tests, so a very slow imposed deformation of the material, in order to give hydrogen necessary time
 53 to hydrogen to concentrate in the plastic zone; on the other hand there was the study of static behavior
 54 of materials investigated by means of Four Point Bending Tests.

55 In addition, a permeation test campaign was performed to evaluate the diffusion coefficient and its
 56 dependence on thermal treatment.

57 The aim of this activity was to determine a practical and easy-applicable methodology to study the
 58 susceptibility to hydrogen of Ultra High Strength Steels for automotive industry.

59 2. Materials and Methods

60 2.1. Materials

61 The material under investigation [2] is a patented ultra-high strength Aluminum-Silicon coated boron
 62 steel. Two grades were studied, one with 1500 MPa of UTS and one with 2000 MPa.

63 These materials are subjected to hot forming process and they are used in structural and safety
 64 automobile components.

65 After the thermal treatment the microstructure is completely martensite and thus susceptibility to
 66 hydrogen embrittlement increases.

67

68

69

Table 1 Chemical compositions of the two steels (wt %)

	C	Si	Mn	P	S	Al	B	Ti	Cr
USIBOR 1500 ®	0,19	0,21	1,13	0,015	0,008	0,0038	0,003	0,031	0,19
USIBOR 2000 ®	0,38	0,19	1,21	0,013	0,006	0,032	0,0032	0,024	0,28

70

71

Mechanical properties of the two materials are shown in Table 2:

72

73

Table 2 Mechanical properties of materials under investigation

	R _{P,02} [MPa]	R _m [MPa]	A ₅₀ [%]
1500 Grade	1252	1485	7,3
2000 Grade	1510	1881	6,2

74

75

The difference in mechanical properties has to be imputed to a major content of C in USIBOR 2000

76

®.

77 2.2. Hydrogen Charging

78 A charging by electrochemical way was achieved, immersing the samples in a solution and imposing
 79 a current between cathode (the sample) and anode (platinum mesh) simulating the cataphoresis
 80 process. Used solutions containing NaCl and NH₄SCN [3], the variation and combination of current
 81 and solution's composition, in particular in terms of recombination's poison, allowed to vary the
 82 hydrogen concentration absorbed by the material.

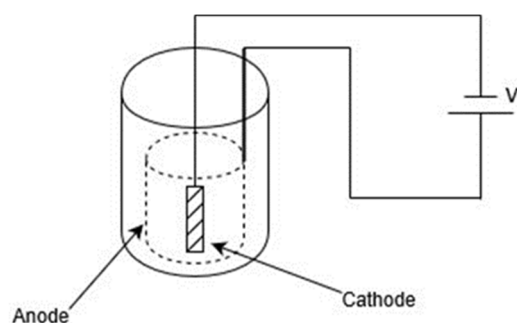
83 In this work NH₄SCN varied in the range of 0,03-0,3 % and current in the range of 0,25-1 mA/cm² to
 84 avoid surface damage.

85 Every sample was further treated by introducing it in the laboratory furnace and heating material at
 86 the temperature of 150 °C for 10 minutes simulating paint baking industrial process: in this way a

87 uniform hydrogen distribution was achieved inside the material and, according to [4], not a
 88 considerable amount of hydrogen was desorbed.

89 In Figure 1 the electrochemical device for hydrogen charging is depicted:

90
 91



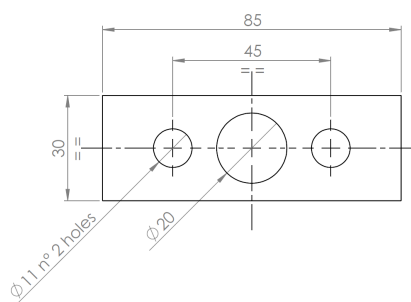
92
 93

Figure 1 Electrochemical cell for hydrogen charging

94 2.3. Slow Strain Rate Tests

95 The slow strain rate tests were performed referring to ASTM G129 [5] setting a crossbar velocity of
 96 0,001 mm/s; the very slow rate corresponds to a very low deformation rate: in this way hydrogen is
 97 able to migrate towards the following fracture zone.

98 The geometrical and dimensional characteristics according to [6] of the sample used in these tests are
 99 shown in Figure 2:



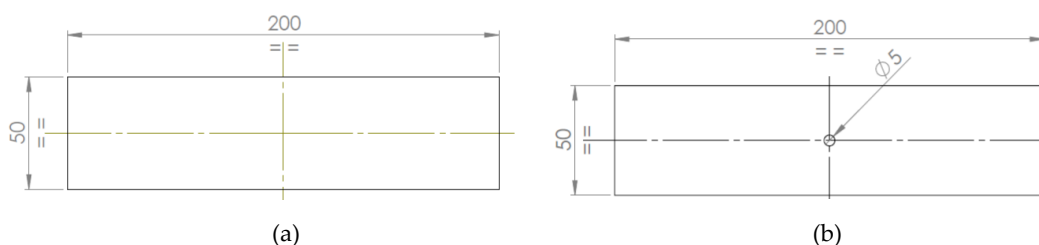
100
 101

Figure 2 SSRT sample

102 2.4. Four Point Bending Tests

103 The experimental method provided four point bending (4PB) tests to evaluate the susceptibility of
 104 the steel to delayed fracture due to hydrogen; 4PB tests were carried out referring to ASTM F-1624
 105 [7]; the dimensions of samples used in those tests are represented in
 106 Figure 3.

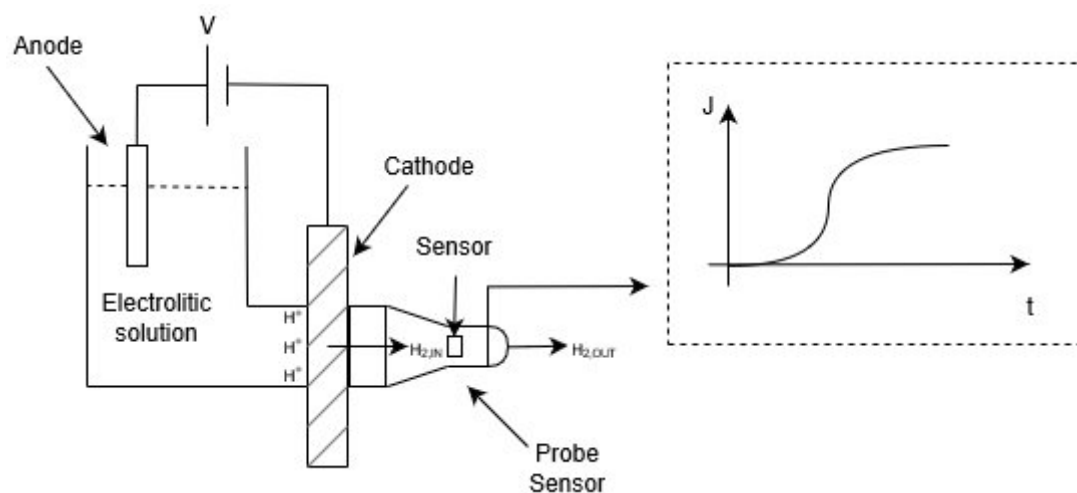
107



107

Figure 3: Dimensions and geometry of (a) four point bending test samples without hole and (b) with

109 The loading consists of increasing the stress to which the material is subjected progressively, always
 110 in the elastic range, starting from 50% of $R_{p,0.2}$; this load was maintained for 24 h, then it was
 111 increased every 2 hours up to 90%.



140

141

Figure 5 Innovative instrument patented by Letomec S.r.l

142

143 2.5. Hydrogen Measurement

144 For 4PB and SSR tests the concentration of hydrogen was evaluated by hot extraction method by
 145 means of *Leco* DH603 instrument: samples were heated at 265 °C in order to guarantee the complete
 146 desorption of diffusible hydrogen.

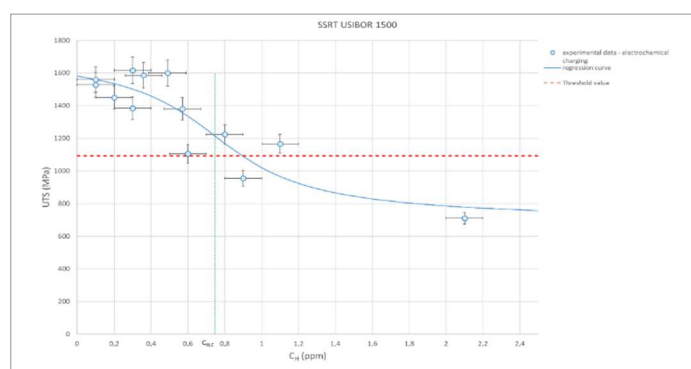
147

148 3. Results

149 3.1. Slow Strain Rate Tests

150 The Slow Strain Rate tests were carried out on hydrogen pre-charged samples : after the sample
 151 fracture the content of hydrogen was measured, details in the previous paragraphs.

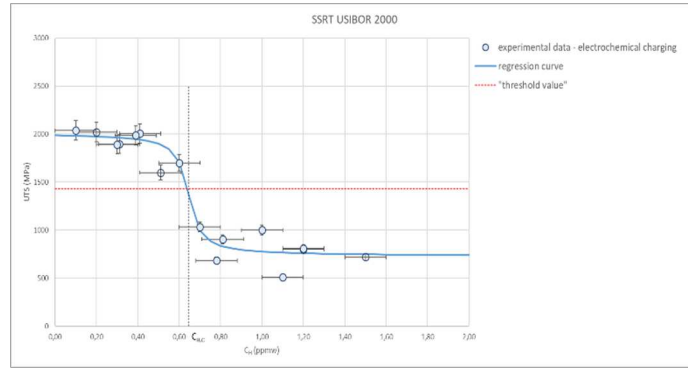
152 In Figure 6 and Figure 7 were reported the two characteristics of the two different materials.



153

154

Figure 6 SSRT for USIBOR 1500 ®



155

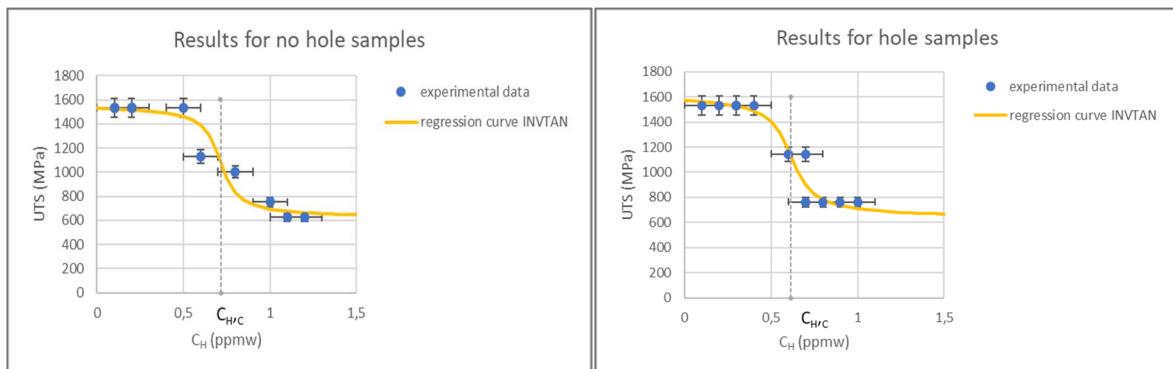
156

Figure 7 SSRT for USIBOR 2000 ®

157 In the figures above, $C_{H,C}$ represents the critical concentration obtained by the inflection point of
 158 the regression curve, correspondent to parameter m_3 . The error bars depend on the sensitivity of
 159 *Leco DH603*, equal to $\pm 0,1$ ppmw while on the y-axis the error value is 5 %, derived from
 160 uncertainty on the measure of the sample's thickness.

161 3.2. Four Point Bending Tests

162 In Figure 8 are shown the 4PB test results for USIBOR 1500 ® while in Figure 9 those related to
 163 USIBOR 2000 ®; the $C_{H,C}$ is again the critical concentration found as the inflection point (and equal to
 164 m_3 in the regression equation); as for the SSR tests the materials presented a first asymptote for low
 165 concentrations, a dramatic fall for a critical concentration and a second asymptote meaning a
 166 saturation effect [11]
 167



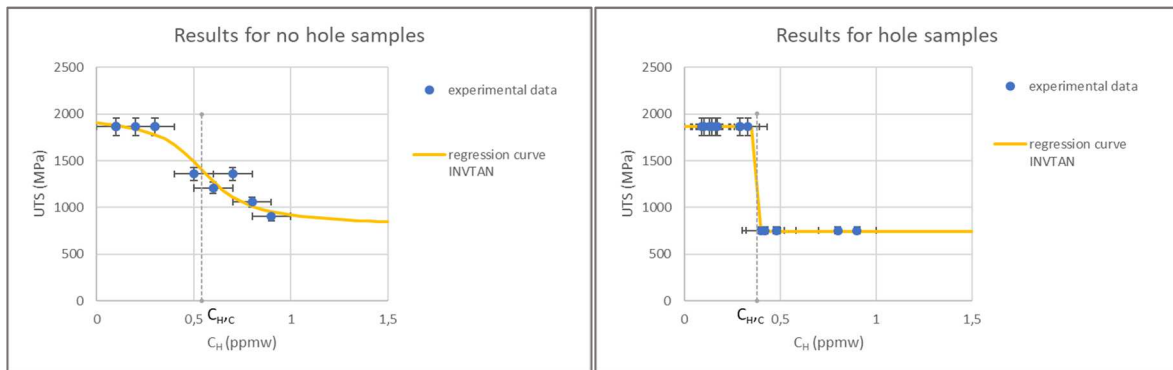
168

169

Figure 8 (a) No hole samples

(b) Hole samples

USIBOR 1500 ®



170

171

Figure 9 (a) No hole samples

(b) Hole samples

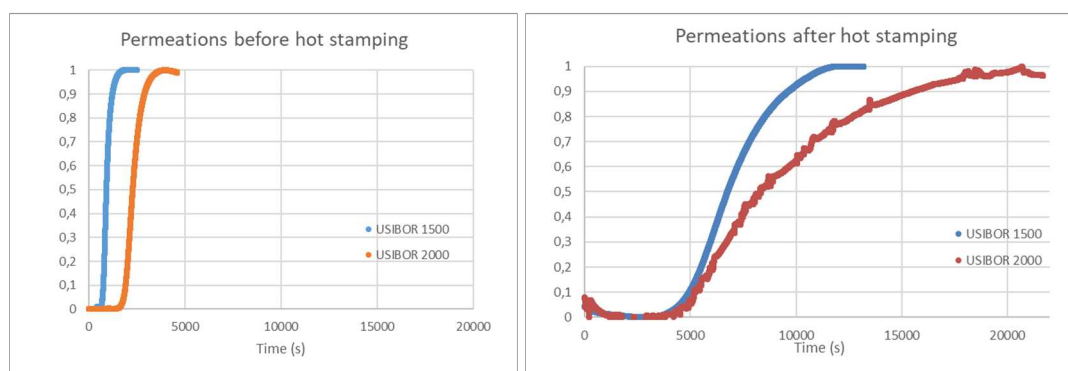
USIBOR 2000 ®

172

173

3.3. Permeation Tests

174 Sample thickness was equal to 1,4 mm in this particular case for both materials, the two steels were
 175 both undergone to permeation tests before and after hot stamping treatment to study the effect of
 176 microstructure transformation. In Figure 10 are compared the results:



177
 178 **Figure 10:**(a) Permeations cure before hot stamping (b) Permeations curve after hot stamping

179 As said before, in Table 3 are shown the diffusion coefficients for the two different materials under
 180 investigation: according to international literature [12], the differences underlined before are
 181 evident.

182
 183

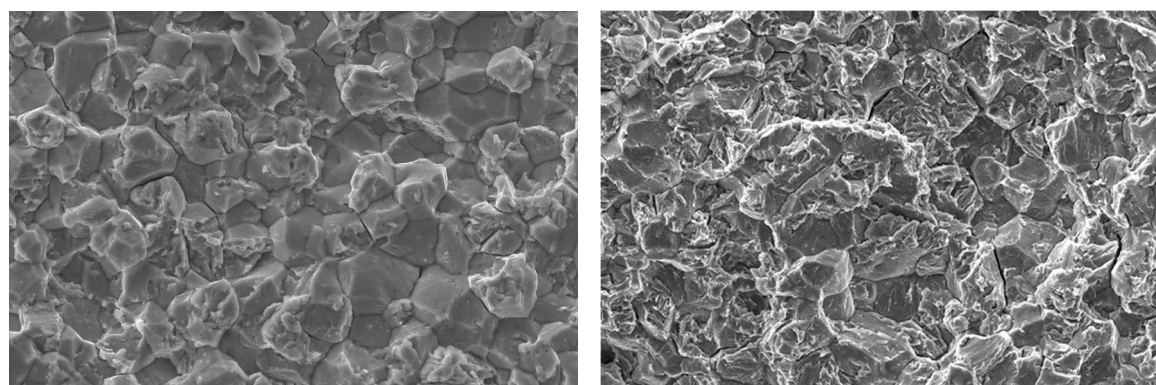
Table 3 Diffusion coefficient for the two grades steels as a function of thermal treatment

	Diffusion coefficient (m ² /s)	
	Before Hot Stamping	After Hot Stamping
1500 Grade	3,39E-10	4,50E-11
2000 Grade	1,36E-10	3,25E-11

184
 185

3.3. SEM Images

186 In Figure 11 SEM images are shown and typical intergranular fracture surface is illustrated:



187
 188 **Figure 11** (a) USIBOR 1500 ® (b) USIBOR 2000 ®

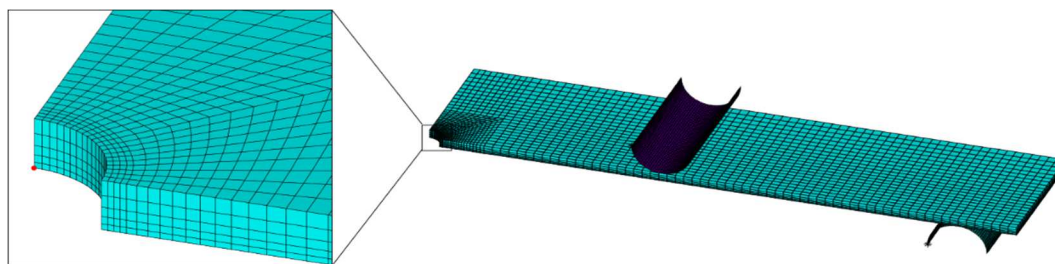
189 For both pictures the magnification is 5000x and the hydrogen content, absorbed by the samples,
 190 was 2,1 ppmw and 0,5 ppmw, respectively.

191

192 3.4. FEM Simulation

193 The FE model was simplified representing a quarter of the sample considering symmetry planes.
 194 Loading cylinders and sample were linked together with contact elements, which allowed the
 195 contact region to move in function of the deformed shape, taking into account the non-linearity of
 196 geometry (big displacements). For holed specimens FEM simulation returned a stress concentration
 197 factor value close to 2.

198 In Figure 12 is shown the quarter of sample and with a red dot is highlighted the node
 199 correspondent to the maximum of hydrostatic stress.



200

201

Figure 12 FEM images representing point of maximum hydrostatic load (red dot)

202 4. Discussion

203 4.1. Hydrogen diffusion and degradation

204 The diffusion phenomenon is regulated by the Fick's laws and even the movement of hydrogen
 205 atoms inside a steel can be described by means of Fick's equations. Experimental tests
 206 demonstrated a behaviour a little far from the ideal theory: this difference is due to the presence of
 207 hydrogen traps inside the metals lattice such as dislocations, grain boundaries, precipitates and so
 208 on.

209 Traps influence the diffusion of atoms in the bulk and they are divided in two categories: reversible
 210 and irreversible, depending on their own binding energy related to the traps (irreversible are those
 211 traps that release hydrogen at a temperature higher than 1000 °C while, according to literature, the
 212 reversible hydrogen leaves steel at a lower temperature, in particular for USIBOR it is equal to 265
 213 °C [13]).

214 According to McNabb et al. (1963) model [14], traps saturate and the equations that rule this
 215 phenomenon are shown below [12]:

216

$$217 \begin{cases} \frac{\partial C}{\partial t} = D \frac{\partial^2 C}{\partial x^2} - N_r \frac{\partial v}{\partial t} - N_i \frac{\partial w}{\partial t} \\ \frac{\partial v}{\partial t} = K_r C(1 - v) - pv \\ \frac{\partial w}{\partial t} = K_i C(1 - w) \end{cases} \quad (2)$$

218

219 Where C is the hydrogen concentration (atoms/m³), D the hydrogen diffusion coefficient (m²/s) in
 220 pure iron, N_r and N_i are the concentration of reversible and irreversible traps respectively
 221 (atoms/m³), v represents the occupied reversible traps fraction while w refers to irreversible traps,
 222 t and x the time and space variables; K_r is the trapping rate for reversible traps (m³/atoms s), K_i
 223 is the same for irreversible traps and p is the release rate for reversible traps.

224 As it can be noticed in table 4 and according to [12], traps are dislocations generated from the phase
 225 transformation during the quenching process and the diffusion is always faster in USIBOR 1500 ®

226 than USIBOR 2000® for the major quantity of carbon in the second one; moreover the thermal
227 treatment reduces the diffusion coefficient of hydrogen.

228 The embrittling process [15] is related to the interaction of atomic hydrogen with interatomic bonds
229 and when the cohesive strength of the material is overcome, the crack propagation occurs, referring
230 to the I mode of crack growth according to mechanical fracture. At the crack tip, the presence of a
231 high pressure gradient increases the solubility of hydrogen in the lattice due to lattice expansion,
232 resulting in a hydrogen flux towards this region.

233 According to HEDE model the cohesive strength is affected only by lattice hydrogen C_L and its
234 dependence is shown in the following equation:

$$235 \sigma_N^c(C_L) = \sigma_N^c(1 - a_1\theta_s + a_2\theta_s^2) \quad (3)$$

238 With a_1 and a_2 empirical constants and θ_s defined as:

$$240 \theta_s = \frac{C_L}{C_L + \exp\left(-\frac{\Delta H}{RT}\right)} \quad (4)$$

241 Where ΔH is equal to 30 kJ/mol, R the gas constant and T absolute temperature.

243 The hydrogen concentration tends to accumulate next to the crack tip because of higher hydrostatic
244 stresses, according to the well known Beck's law [16]:

$$245 C = C_L \exp\left(\frac{V_H \sigma_H}{RT}\right) \quad (5)$$

246 Where V_H is the molar volume of hydrogen in the lattice, equal to 2E-06 m³/mol, σ_H is the
247 hydrostatic tension, R the gas constant, T the absolute temperature, C_L the concentration of
248 hydrogen without stress and C the concentration near the crack tip in presence of stress [17].
249 The accumulation of hydrogen in potential cracking initiation sites depends on the strain-stress
250 time gradient and diffusion coefficients [18]:

$$252 \frac{\partial C}{\partial t} = D \nabla^2 C + D \frac{V_H}{R(T - T^z)} \nabla C \nabla p + D \frac{V_H}{R(T - T^z)} C \nabla^2 p \quad (6)$$

253 Where C is the hydrogen concentration, D the diffusion coefficient, T^z the absolute zero
254 temperature, p the hydrostatic stress.

256 In international literature it is possible to find various studies of numerical and theoretical simulation
257 in order to explain the hydrogen embrittlement phenomena [18].

258 In automotive industry very thin thickness (0,5-2E-03 m) sheets are used and for this reason a more
259 practical approach is reasonable.

260 The extrapolation of a regression curve, figure 6 and figure 7, able to describe the behavior of the
261 steel[19,20] and the correspondent equation were derived:

$$262 UTS (MPa) = m_1 - m_2 \cdot \arctg\left(\frac{C_H - m_3}{m_4}\right) \quad (7)$$

263 From the function's study the point where the second derivative is equal to zero has abscissa equal
264 to $C_H = m_3$ and this is very close to the value of critical hydrogen concentration, obtained
265 according to [21], for both steels.

266 The same was done for the Four Point Bending Tests and from the mathematical expressions,
267 critical hydrogen concentration was found for both materials, summarized in Table 4:

268
269

Table 4 Critical Hydrogen Concentration for the different mechanical tests

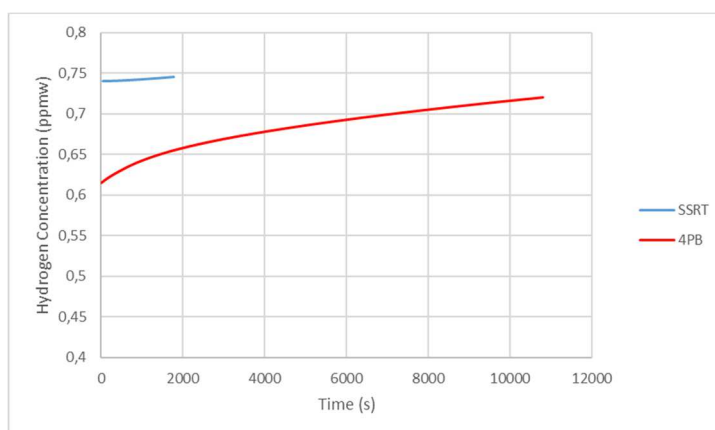
USIBOR 1500®	USIBOR 2000®
--------------	--------------

4PB Hole	0,61	0,37
4PB No Hole	0,71	0,54
SSRT	0,74	0,64

270

271 The worst conditions are given by the presence of hole in 4PB samples; differently from the SSR
 272 specimens where the deformation rate is higher than the diffusion and the hole creates an intensity
 273 factor really near to 1: for this reason, the accumulation of hydrogen in the SSR sample is negligible
 274 while a more emphatic effect can be noted in the 4PB with hole. The 4PB without hole samples
 275 showed a concentration closer to SSRT specimens, even though the difference in test time duration,
 276 due to the absence of stress gradient.

277 In Figure 13 is represented the evolution of hydrogen concentration at the crack tip as a function of
 278 test time.



279

280 **Figure 13** Hydrogen accumulation at the crack tip during the test. Note: simulation is related to USIBOR 1500®

281 5. Conclusions

282 From the different mechanical tests on USIBOR 1500 ®and USIBOR 2000 ®, the following conclusions
 283 can be summarized:

- 284 • These steels are sensitive to the hydrogen delayed fracture and the grade 2000 is quite more
 285 sensitive than grade 1500.
- 286 • The 4PB tests with hole are the most severe because the failure occurs with a minimum
 287 average concentration.
- 288 • The hydrogen diffusion strongly decreases after hot stamping and quenching process
 289 because of the martensite formation; moreover, because of the higher amount of carbon,
 290 grade 2000 has a slower diffusion.
- 291 • The differences in critical hydrogen concentration values for the mechanical tests is due to
 292 two factors:
 - 293 1. The effect of deformation rate in the SSRT that gives a minor time to hydrogen to
 294 diffuse near the crack tip.
 - 295 2. The presence of the hole in the 4PB samples induces tension gradients that, coupled
 296 to time, create hydrogen accumulation near the crack tip.
- 297 • Finally, the 4PB with hole is absolutely the most realistic test to simulate the risk of hydrogen
 298 embrittlement for this type of materials; however the SSR test can represent a quick method
 299 to compare different materials behavior in presence of hydrogen.

300 **Author Contributions:** S.C., R. V. and M.V. designed and conceived the experiments; M.V., S.C. and L.B.
 301 performed the experiments; all the authors analyzed data; M.M.T. provided materials; M.V. and R.V. wrote the
 302 paper.

303 **Acknowledgments:** Authors desire to thank Eng. Barile and Eng. Thierry (Arcelor Mittal) for materials; Prof.
 304 Bernardo Monelli and PhD student Francesco Aiello for FEM simulation.

305 **Conflicts of Interest:** The authors declare no conflict of interest.

306 **References**

- 307 1. Djukic, M.B., Sijacki Zeravcic, V., Bakic, G.M., Sedmak A., Rajcic B. Hydrogen damage of steels: A
308 case study and hydrogen embrittlement model. *Eng. Fail. Anal.* **2015**, *58*, 485-498
309 [http://dx.doi.org/10.1016/j.engfailanal.2015.05.017].
- 310 2. Arcelor Mittal, Available online: https://automotive.arcelormittal.com/usibor_ductibor
- 311 3. Takaji S., Toji Y. Application of NH₄SCN Aqueous Solution to Hydrogen Embrittlement Resistance
312 Evolution of Ultra-High Strength Steels. *ISIJ Int.* **2012**, *52*, 329-331
313 [http://dx.doi.org/10.2355/isijinternational.52.329].
- 314 4. Kim, H.J., Park, H.K., Lee, C.W., Yoo, B.G., Jung, H.Y. Baking Effect on Desorption of Diffusible
315 Hydrogen and Hydrogen Embrittlement on Hot-Stamped Boron Martensitic Steel. *Metals* **2019**, *9*, 636
316 [doi:10.3390/met9060636].
- 317 5. ASTM G129: 2000, Standard practice for slow strain rate testing to evaluate the susceptibility of
318 metallic materials to environmentally assisted cracking.
- 319 6. SEP 1970: 2011, Test Of The Resistance Of Advanced High Strength Steel (AHSS) For Automotive
320 Applications Against Production Related Hydrogen Induced Brittle Fracture.
- 321 7. ASTM F1624: 2018, Standard Test Method for Measurement of Hydrogen Embrittlement Threshold
322 in Steel by the Incremental Step Loading Technique.
- 323 8. ISO 17081:2004 , Method of measurement of hydrogen permeation and determination of hydrogen
324 uptake and transport in metals by an electrochemical technique.
- 325 9. Valentini, R. (Letomec srl), PATENT EP2912452, **2012**.
- 326 10. Lasia, A., Gregoire D. General Model of Electrochemical Hydrogen Absorption into Metals. *J.*
327 *Electrochem. Soc.* **1995**, *142*, 3393-3399 [doi: 10.1149/1.2050267].
- 328 11. Lovicu, G., Bottazzi, M., D'Aiuto, F., De Sanctis, M., Di Matteo A., Santus, C., Valentini, R. Hydrogen
329 Embrittlement of Automotive Advanced High-Strength Steels. *Metall. Mater. Trans.* **2012**, *43A*, 4075-
330 4087 [https://doi.org/10.1007/s11661-012-1280-8].
- 331 12. Cherubini, A., Bacchi, L., Corsinovi S., Beghini, M., Valentini, R. Hydrogen Embrittlement in
332 Advanced High Strength Steels: a new investigation approach. 22nd European Conference on Fracture,
333 Belgrade, Serbia, 26-31 August 2018; Elsevier [https://doi.org/10.1016/j.prostr.2018.12.125].
- 334 13. Georges, C., Sturel, T., Drillet, P., Maigne J.M. Absorption/Desorption of Diffusible Hydrogen in
335 Aluminized Boron Steel. *ISIJ Int.* **2013**, *53*, 1295-1304 [https://doi.org/10.2355/isijinternational.53.1295]
- 336 14. McNabb, A., Foster, P.K. A new analysis of the diffusion of hydrogen in iron and ferritic steels. *Trans.*
337 *Metallurgical Soc. AIME* **1963**, *227*, 618-627.
- 338 15. Brocks, W., Felkenberg, R., Scheider, I., Coupling aspects in the simulation of hydrogen-induced stress
339 corrosion cracking. *Procedia IUTAM* **2012**, *3*, 11-24 [https://doi.org/10.1016/j.piutam.2012.03.002].
- 340 16. Beck, W., Subramanyan, P.K., Williams, F.S. Interpretation of Some Hydrogen Embrittlement
341 Phenomena. *Corrosion* **1971**, *27*, 115-118 [doi:10.5006/0010-9312-27.3.115].
- 342 17. Fu, L., Fang, H., Formation Criterion of Hydrogen-Induced Cracking in Steel Based on Fracture
343 Mechanics. *Metals* **2018**, *8*, 940 [doi:10.3390/met8110940].
- 344 18. Olden, V., Alvaro, A., Akselsen, O.M., Hydrogen diffusion and hydrogen influenced critical stress
345 intensity in an API X70 pipeline steel welded joint-Experiments and FE simulations. *Int J Hydrogen*
346 *Energ* **2012**, *37*, 11474-11486 [DOI: 10.1016/j.ijhydene.2012.05.005].
- 347 19. Valentini, R., Tedesco, M.M., Corsinovi, S., Bacchi, L. Delayed Fracture in Automotive Advanced
348 High Strength Steel: A New Investigation Approach. *Steel Res. Int.* **2019**, (accepted)
349 [https://doi.org/10.1002/srin.201900136].
- 350 20. Beghini, M., Benamati, G., Bertini, L., Recapito, I., Valentini, R., Effect of hydrogen on the ductility
351 reduction of F82H martensitic steel after different heat treatments *J. Nucl. Mater* **2001**, *288*, 1-6.
- 352 21. Pressouyre, G.M., Faure, F.M. Quantitative Analysis of Critical Concentrations for Hydrogen Induced
353 Cracking. Second National Symposium on Test Methods for Hydrogen Embrittlement: Prevention
354 and Control, Los Angeles, California, 24-26 May 1985, ASTM [https://doi.org/10.1520/STP45314S].
355

